Toward the development of a LES-SGS closure model for buoyant plumes

By S. R. Tieszen †, H. Pitsch, G. Blanquart AND S. Abarzhi

LES simulations of a helium plume based on a dynamic Smagorinski closure model show very strong grid dependency. The authors interpret these results as the inability of diffusive, eddy-viscosity closure models to capture the growth of Rayleigh-Taylor (RT) instabilities, which develop at the plume-air interface, create thin finger-type structures, and lead eventually to strong mixing of air and helium. To capture the RT mixing and to achieve grid independent results, unreasonably high grid densities are required. Our motivation is therefore to develop subgrid models, which could reproduce the robust effect of the RT mixing on the plume dynamics, without having to capture the details of dynamics at small-scales. Preliminary results from a developed model highlight difficulties and suggest directions for future study.

1. Introduction

1.1. *Motivation and Objectives*

This study is motivated by the need to simulate large, turbulent, reacting plumes, i.e., fires. For fully turbulent fires, the ratio between the height and diameter is on the order of O(2) (Drysdale 1999). Therefore, significant turbulent mixing occurs within the first diameter of a fire. Understanding and predicting this mixing is critical to modeling a fire. Subgrid combustion and soot models are critically dependent on relevant scalar fields and subgrid mixing rate estimates. These models in turn strongly affect the density field and the fields for effective radiative properties. The radiative properties strongly affect heat transfer to fuel sources that sustain the fire. Fundamentally, reactive scalars couple to momentum through three primary pathways, the momentum source term through variable density, advection through dilatation via the continuity condition and the density, and diffusion through changes in viscosity. While all three couplings are present in all reacting flows, fires, as reacting plumes, are very strongly affected by the source term coupling. Due to its importance, it is of interest to study the source term coupling independently from the other couplings. The effects of variable density can be achieved through species alone. In a fire, peak density ratios between reaction zone products and ambient air are of O(7). The density ratio of helium and air is of the same order. For this reason, an iso-thermal helium plume will be used to assess subgrid model requirements to capture the momentum source term coupling for buoyant plumes. The scope of this study is limited to a comparison with experimental data from O'Hern *et al.* (2004) for a 1 meter diameter helium plume.

1.2. *Literature Review*

Relatively few numerical studies are specifically focused on the near source region of plumes. One reason for this lack of studies is that, until recently, there has been very

† Sandia National Laboratory

little plume data available to compare with simulations. Much of the plume literature has focused on the rate at which a plume will become self-similar (elevation/diameter $\gg 2$) and thus is not relevant to the current study. Further, much of the data is derived from buoyant jets that are buoyant in the far field but momentum dominated in the near source region. In addition to the one meter diameter study used here, transient laminar data are available from Cetegen 1997 and data from a moderately turbulent buoyant plume ($Ri = 2.6$, $Re = 291$) are available from Mell 2001.

The most relevant numerical study of the near source region of non-reacting buoyant plumes is the LES study of DesJardin *et al.* 2004. This study demonstrated significant grid dependency of the results with the use of a dynamic Smagorinski model, and concluded that the best results were obtained with the model turned off. The nature of the turbulence was not identified, but it was suggested by the authors that the under-resolution of the sharp density gradients could result in an underprediction of vorticity in the plume. A study by Tieszen *et al.* 2004 using temporally filtered equations with a narrow temporal filter width (relative to the puffing frequency) and a modified $k - \epsilon$ closure model also showed strong grid dependency. The strong grid dependency resulting from these studies clearly indicates that dissipative, eddy viscosity type closures are insufficient descriptions of the turbulent mixing process. LES studies have also been conducted on reacting plumes, i.e., fires, (Xin *et al.* 2002;Mell *et al.* 1996;Tieszen *et al.* 1996). Mell *et al.* 1996 notes that in addition to hydrostatic (gravitational) production of vorticity, hydrodynamic production is also important to capture the puffing behavior. Results from all the above mentioned studies indicate that the puffing frequency is determined by large scale phenomena since it can be captured with relatively coarse gridding. However, simulations by DesJardin *et al.* 2004 and Tieszen *et al.* 2004 of a 1 meter diameter helium plume indicate that relatively small-scale, but essentially non-dissipative, turbulent structures can significantly affect the mean flow field.

The above mentioned studies all use primarily dissipative turbulence closure models. While a number of closure models have been developed in the general LES community that capture more physics than just dissipation, these models primarily capture the off-diagonal stresses at the filter cut-off. To the authors' knowledge, no buoyancy specific non-dissipative models have been developed. The LES community has included buoyant production of turbulence in terms of an enhanced eddy viscosity, see for example Eidson T. M. 1985 and Canuto V. M. 1994. Reynolds averaged closure models that include buoyancy also have included it only as an enhanced eddy viscosity (see for for example Nicolette, *et al.* 2004). Clearly there is a need for the development of a buoyant turbulent model that captures key non-dissipative physics.

It is well known that the near source region of plumes and fires are dominated by puffing (Cetegen & Ahmed 1993). The nature of the instability (absolute or convective) that results in puffing is a matter of some discussion (Tieszen 2001). Recent studies strongly argue that, while complicated, the instability is absolute (Soteriou *et al.* 2002). Previous studies on both Rayleigh-Taylor (RT), (Duff *et al.* 1962;Dimonte & Schneider 2000;Debacq *et al.* 2001) and Kelvin-Helmholz (KH) (Wang 1984) instabilities are relevant to the current study. The helium plume entering vertically into air in earth's gravity field can be thought of as a classical RT problem with the complications of finite boundary conditions. The finite boundary conditions give rise to the coherent vertical plume; the large scale dynamics of which are dominated by puffing.

The current study employs a well established LES code to compare with helium plume experimental results. The comparison is described in the next section. The dynamics of

the turbulence are subsequently discussed, from which subgrid modeling approaches and requirements are derived. The relevance of the helium plume to fires is discussed and conclusions are drawn in the final section.

2. Data and LES Comparisons

2.1. *Experimental and Numerical Details*

The two-dimensional data available from O'Hern *et al.* (2004) consists of Favre-averaged vertical and horizontal velocities, density, and an estimate of the turbulent kinetic energy on a planar surface passing through the centerline of the 1 meter diameter helium plume source. The lower boundary of the data plane is just above the surface of the source and the upper boundary of the plane is about 0.75 meters above the source. The sides of the plane extend just beyond the plume source to capture edge entrainment into the plume. The laser sheet width is 8 mm. The velocity data are acquired through Particle Image Velocimetry (PIV) and the density data through Planar Laser Induced Fluorescence (PLIF). The inlet plume velocity is 0.34 m/s and the molecular weight of the plume is 5.42 g/mol (due to trace gases required for the PLIF). The plume is issued into air. The temperature is 291 K with an ambient pressure of 82 kPa. Details of the experimental geometry can be found in O'Hern *et al.* (2004). Data uncertainties are: for density $\pm 18\,\%$ of the difference between plume and air density, $\pm 5\,\%$ of the air density, velocities $\pm 20\,\%$, and the turbulent kinetic energy $\pm 30\,\%$.

The current study uses an energy preserving, low mach number LES code (Pierce 2001;Pierce & Moin 2004), unlike the compressible formulation of DesJardin *et al.* 2004 that uses pressure gradient scaling to make the solution affordable, or the non-energy preserving numerics of Tieszen *et al.* 2004. Further, the current study uses a cylindrical formulation of the governing equations on a structured mesh unlike the structured Cartesian solutions of (DesJardin *et al.* 2004) and CVFEM Cartesian solutions of (Tieszen *et al.* 2004). Open boundaries are used except for the floor and inlet. The inlet treatment also differs from the previous studies in that the flow in the diffuser is not specified as a Dirichlet condition, but allowed to develop (ignoring the presence of a honeycomb at the exit).

2.2. *Grid Sensitivity Results*

For grid sensitivity studies, a dynamic Smagorinsky model was used to close the momentum equations. A mixture fraction equation was solved for the helium mass fraction. Its closure model consists of a gradient-diffusion assumption. Since previous studies showed strong mesh sensitivity, simulations were conducted with three mesh densities. A coarse mesh of nominally 250 K nodes (r, θ, z: $52 \times 64 \times 80$), a medium mesh of nominally 1 M nodes (r, θ, z: $104 \times 64 \times 160$), and fine mesh of nominally 4 M nodes (r, θ, z: $208 \times 64 \times 320$).

Fig. 1 shows contours of plume density at an instant in time. The transient results are time averaged after a quasi-steady puffing mode has been achieved. The time-averaged results are shown in Fig. 2 through 5. Figure 2 shows the time-averaged density contours. As the mesh density is increased from 250 K to 1 M to 4 M, more air is mixed into the plume. increasing the centerline density. Comparing the centerline density between the simulations and the data, a monotonic trend is seen, in which the results of the simulation approach the data as the mesh density is increased.

As seen in Fig. 3, an over-prediction of the centerline vertical velocity occurs for under-resolved meshes. However, as the mesh density is increased the results of the simulation

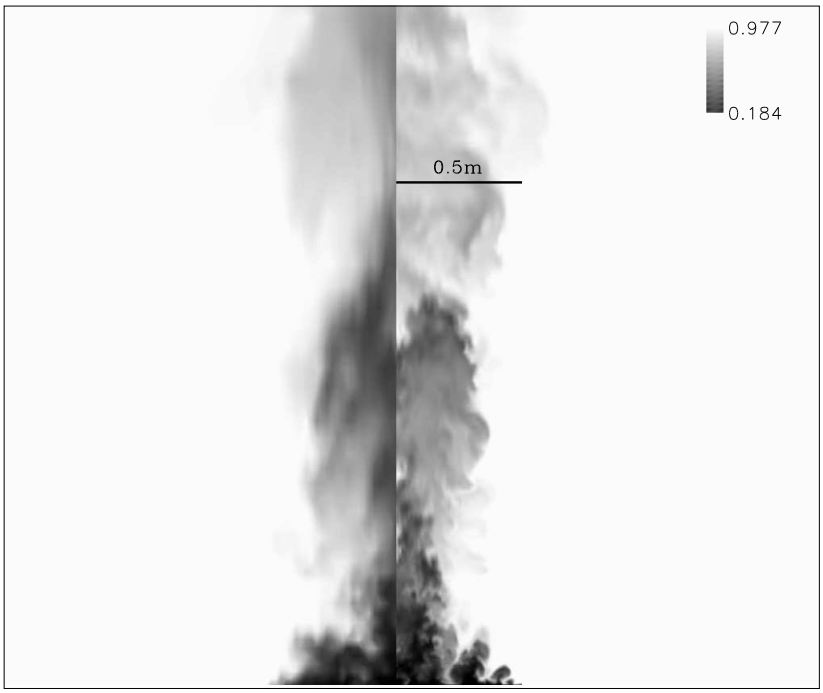

FIGURE 1. Density Contours for a Typical Time Plane. Left Side - 250 K node simulation. Right Side - 4 M node simulation.

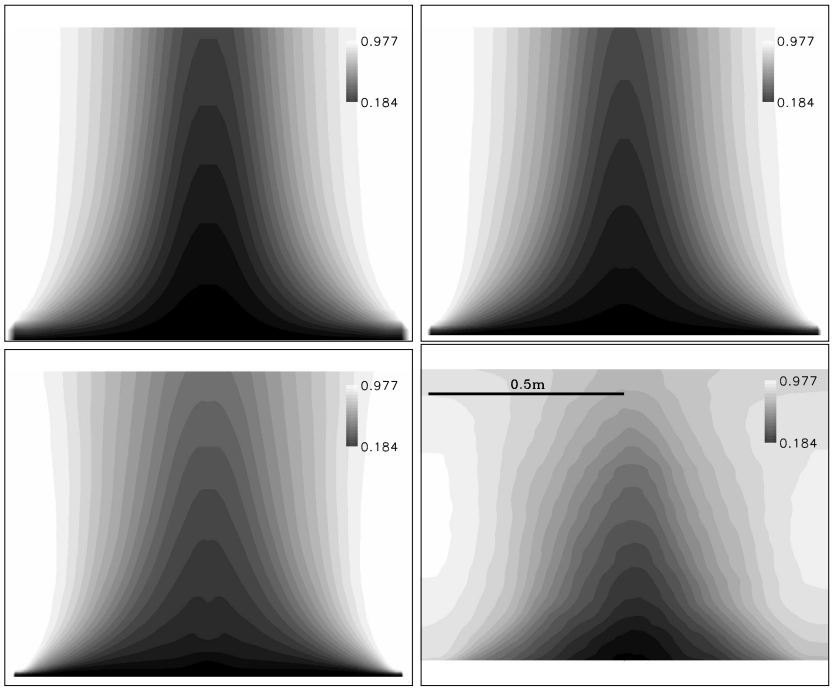

FIGURE 2. Density. Comparison between data (lower right) and simulations with 250 K (upper left), 1 M (upper right) and 4 M nodes (lower left).

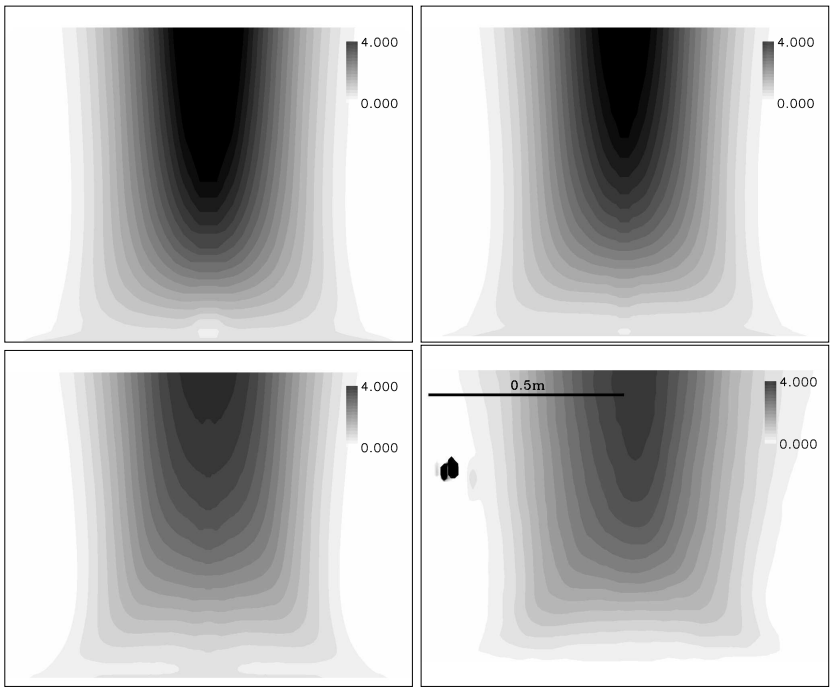

FIGURE 3. Vertical velocity (m/s). Comparison between data (lower right) and simulations with 250 K (upper left), 1 M (upper right) and 4 M nodes (lower left).

approach the data. The centerline velocity overshoot is consistent with the centerline density undershoot at a given mesh density. Both indicate that there is not enough scalar mixing occurring within the plume for the under-resolved simulations. Figure 4 shows the horizontal velocity contours for the simulations and the data. The radial velocity shows relatively little sensitivity to mesh density. This result is somewhat surprising, since continuity must be preserved and there is a relatively large difference in the vertical centerline velocities with mesh density. Comparing Fig. 4 with Fig. 2, it can be seen that the peak velocities occur in a region of high density gradients and the small changes in the locations of the velocity peaks can account for the lack of large changes in the velocity magnitude with grid density. Figure 5 shows the turbulent kinetic energy for the simulations and the data. Since only two-dimensional PIV data was experimentally available, an assumption was made in data processing that the out-of-plane horizontal velocity fluctuations are equal to the inplane horizontal velocity fluctuations. To be consistent, the numerical simulation data is processed in the same fashion. The under-resolved simulations result in too much turbulent kinetic energy along the centerline. Since the turbulent kinetic energy is dominated by the large scale puffing phenomena, this result indicates that the puffs are too strong. A lack of mixing also accounts for this result in that the velocities are too high, and the plume is too coherent. As with the mean statistics, the simulation results approach the data monotonically as the mesh density is increased. The choice of a cylindrical formulation also results in a small artifact along the plume centerline.

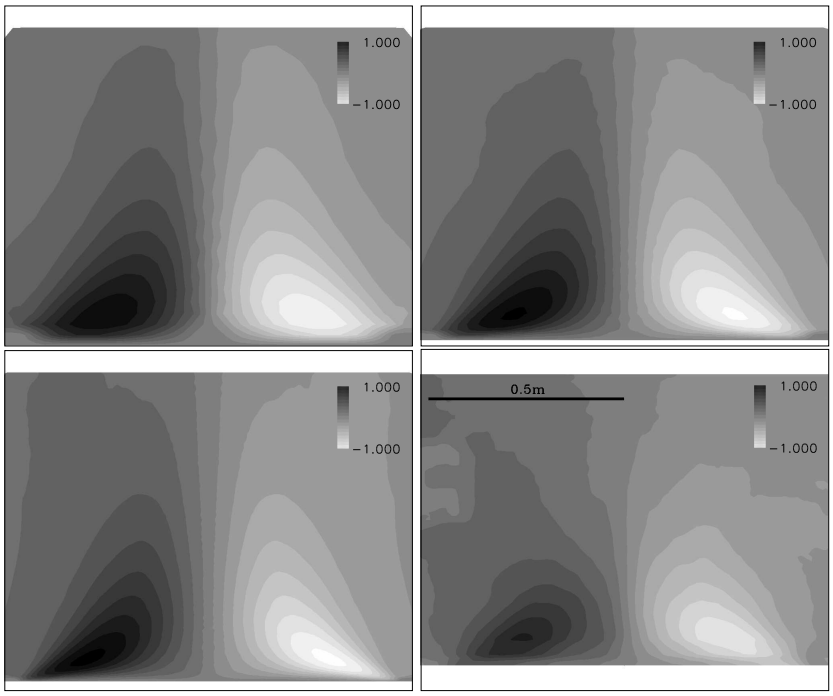

FIGURE 4. Horizontal velocity (m/s). Comparison between data (lower right) and simulations with 250 K (upper left), 1 M (upper right) and 4 M nodes (lower left).

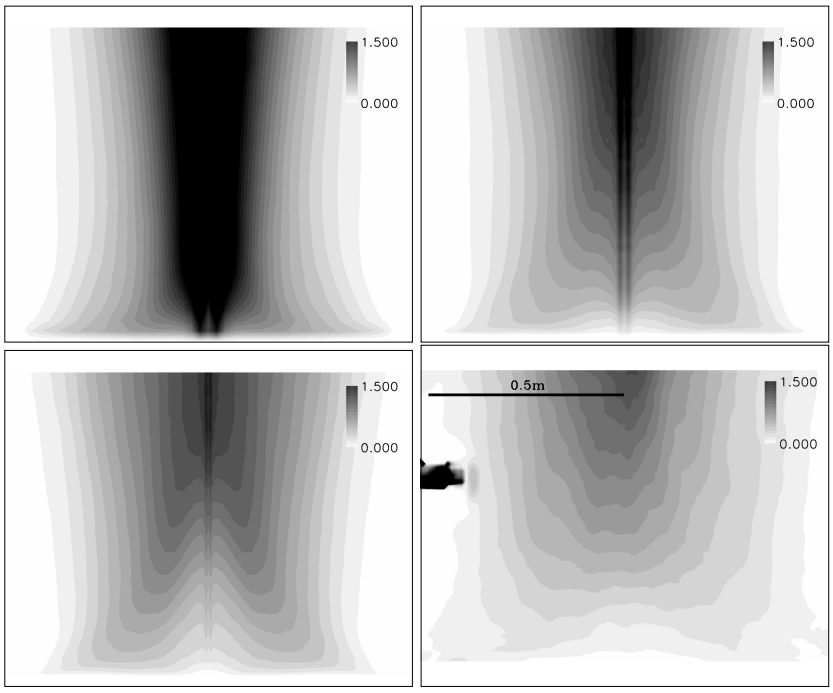

FIGURE 5. Turbulent Kinetic Energy (m^2/s^2). Comparison between data (lower right) and simulations with 250 K (upper left), 1 M (upper right) and 4 M nodes (lower left).

3. Turbulent Dynamics and Subgrid Model Requirements

3.1. *Near Plume Source Laminar Instability Dynamics*

The grid refinement study compares favorably with the results of DesJardin *et al.* 2004 and Tieszen *et al.* 2004. All studies used different numerics, but all of them use only diffusive, eddy-viscosity type turbulence closure models and all show similar results with strong grid dependencies. The results suggest that the under-resolved turbulent structures are doing more than just dissipating energy. Scalar mixing is clearly being affected in a manner which significantly alters the time-averaged statistics. As the grid is refined, more of the mixing is picked up by the increased grid resolution, resulting in more mixing in the plume. Thus, simple dissipative closures like the dynamic Smagorinski model are not capturing the turbulence mechanisms that result in the mixing for this plume. In order to postulate a model that can capture the mixing physics, it is necessary to understand the mechanisms which govern mixing in the near field of a plume.

Based on the phenomenological arguments, simulations results, and the transient data, an argument can be made that the mixing mechanism that is not being resolved with coarser grids is the growth of Rayleigh-Taylor instabilities. In a buoyancy dominated flow, it is the density difference between the plume and the surroundings that is the driving force for the flow, as can be seen in the time-averaged simulation results. As the simulation results approach the correct density profile with increased grid resolution, all velocity and turbulence statistics approach the data. These results suggest that resolving the circulation evolution is sufficient to resolve the flowfield. A circulation evolution equation, derived from the vorticity transport equation, (Najm *et al.* 1998) is given by

$$\frac{d}{dt}\Gamma = \int_A dA \bullet \left[\frac{1}{\rho}\nabla\rho \times \left(\frac{1}{Fr}g - \frac{D\mathbf{v}}{Dt}\right) + \frac{1}{Re}\frac{\nabla \times \Phi}{\rho}\right]. \tag{3.1}$$

The right hand side of Eq. 3.1 is the motive force for circulation. It implies that it is not necessary to resolve the density gradients to capture the evolution of circulation. It is only necessary to capture density differences normal to the local acceleration field. In other words, for a given discretization, if the cell density is correct for each cell, then the true subgrid density distribution need not be known for circulation to be properly represented. The key is to resolve spatial density fluctuations at the scale they occur. Note that scalar fields are a result of the time history of the flow field, not just the local instantaneous turbulence intensities.

Scalar structures exist across a broad range of scales in a plume. The largest scalar structures are the large toroidal puffs that characterize all plumes, as seen in Figure 1. These large scalar structures are the consequence of the vorticity generated at the edge of the plume and grow from relatively small eddies near the toe of the plume due to the persistency of the density gradient at the plume edge. Figure 6 shows distinct scalar structures that are a result of the mixing caused by the growth of laminar instabilities in the near source region of the flow. The helium bubble and air spike structures will continue to grow until they are rolled up into the large toroidal eddies as part of the puff cycle. A consequence of these dynamics is that air from the RT bubbles and spikes gets swept into the centerline early in the plume development.

The relevant scale of the RT instability can be estimated on the basis of dimensional grounds (Duff *et al.* 1962) which suggests

$$\lambda = \left(\frac{D^2}{Ag}\right)^{\frac{1}{3}} \tag{3.2}$$

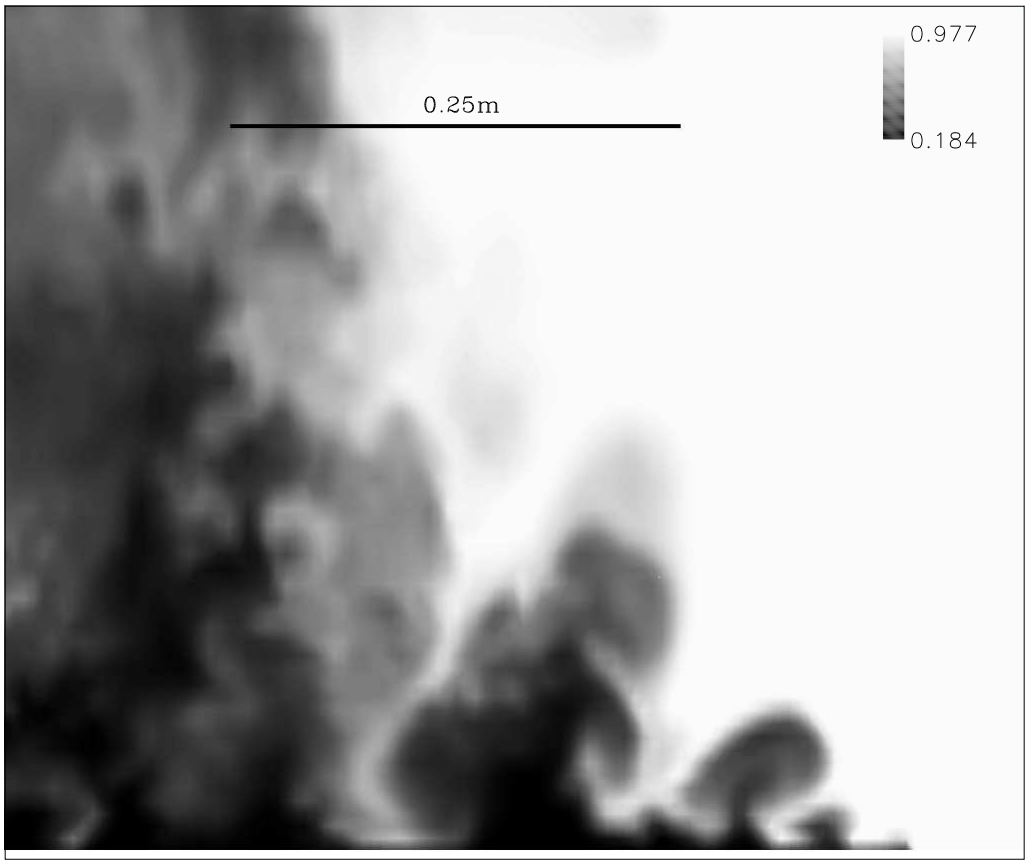

FIGURE 6. Density Contours Near the Plume Source showing Rayleigh-Taylor Bubbles and Spikes. 4 M node simulation results.

where D is the diffusion coefficient between the plume and air, A is the Atwood number (density difference divided by density sum), and g is gravity. For the helium plume (molecular weight = 5.42 g/mol), the Atwood number is 0.685 and D is approximately $7.1\text{x}10^{-5}\ m^2/s$. For these conditions, the fastest growth mode is O(mm). Equation 3.2 is for unforced growth. The scale can be different if the flow is forced, as is possible with all the turbulent instabilities present in the helium plume. The experimental images suggest that the actual air spikes are more like O(cm) wide and somewhat laminar in nature.

RT studies show that in the nonlinear phase of the instability, the amplitude growth is dominated by the characteristic width of the RT structures, i.e. by the horizontal length scale, and it is linear with time (compared to the square of time for turbulent flow dominated by vertical length scales). The amplitude can be approximated by

$$H = \frac{t}{2}\sqrt{gL}\left(\sqrt{\frac{2A}{1+A}} + \sqrt{\frac{2A}{1-A}}\right), \tag{3.3}$$

where t is the growth time and L is the characteristic width of the RT structures, (Dimonte & Schneider 2000).

Dynamically, the RT structures form during the phase of the puff cycle when there is air over the top of the rising helium plume. This phase of the cycle occurs after the large

coherent vortices associated with a puff pull air in over the top of the helium and begin to advect away. As the helium moves into the air, the classical bubble and spike structure begins to form. While the width of the air spikes remains O(cm), the persistence of the density difference between the upward rising bubbles and the downward sinking spikes results in a scalar field in which the scalar structures are much taller than the scale of the laminar instability that creates them. As a first approximation, it can be considered that RT instability persists for about 1/2 the puff cycle period. The puffing period for this plume is 0.7 seconds based on O'Hern *et al.* (2004), so t can be taken as approximately 0.35 seconds. Using 1 cm as the characteristic width of the RT structure, the height of the structure can reach O(15 cm) according to Eq. 3.3. This distance is consistent with the structures shown in Fig. 6. The RT growth period ends when vortices formed at the edge of the plume grow strong enough to result in the radial indraw of air. This indraw temporarily cuts off the helium and advects the RT structures up into the core of the plume. The cycle then repeats itself.

The Ph.D. thesis of Wang 1984 is also relevant to the current study. Wang studied curved shear layers with various density ratios. A close comparison of Fig. 2 and 3 shows that there is not a strong velocity difference across the path of strongest density gradient. Hence the Kelvin-Helmholtz instabilitiy is not strong for this flow. However, the flow transitions from nearly horizontal to nearly vertical with a mean velocity of O(2 m/s). Given a radius of curvature of approximately a plume radius, the centripetal acceleration is on the same order as gravity. The heavy fluid, air, is on the inside of the curved interface with the light fluid, helium, on the outside of the curved interface. Wang 1984 shows experimentally under similar conditions that the RT instability dominates the mixing.

3.2. *Model Development Paths*

From these arguments, it can be concluded that it is necessary to build LES closure models that can capture the effect of mixing by the persistent growth of density gradient driven laminar instabilities. It is likely that grid independent DNS can be achieved for this plume if grid densities of O(mm) can be achieved, i.e., $O(10^9)$ node simulations. As the grid resolution is decreased, more and more of the mixing effects have to be modeled. From the results of the current study, it may be possible to achieve grid independent results if a scalar reconstruction method is used to ensure that the density in the spikes is preserved for meshes > 4 million nodes. If the mesh resolution is to be less than several million nodes, it will be necessary to include the effect of mixing due to the spikes, without actually capturing the spike dynamics. Visualization of the more coarsely refined meshes from this study indicated that the spikes were not present (see Fig. 1). This observation is consistent with the time-averaged plume density being too low along the centerline due to lack of air entrainment.

A model form was selected by dimensional and phenomenological reasoning with the intent of capturing the mixing effects of the bubble and spike structure without resolving the dynamics. It is assumed that the dynamic Smagorinski model is sufficient for capturing the standard turbulent subgrid stresses, but to capture the transient laminar growth of RT instabilities an additional closure model would be required. Seen from a grid resolved level, RT instability induced velocities would appear as spatial fluctuating velocities that are driven by density gradients in a gravitational field. Self-correlation would occur in the direction of the RT spike (vertical in the current study) resulting in a single additional term in the gradient of the Reynold stresses that required closure. Using the vertical density gradient and gravity as a measure of the additional unresolved

vertical stress, results in

$$\text{RT Stress Closure Model} = -\frac{\partial}{\partial x_j}\left(f^2 g_k \frac{\partial \rho}{\partial x_k} e_i e_j\right) \quad \text{where} \quad e_i = \frac{g_i}{|g|} \quad \frac{\partial \rho}{\partial x_k} \geq 0 \quad (3.4)$$

where the directional indices permit only the components aligned with the gravity vector. For positive density gradients, this model results in a spreading force along the helium air interface intending to mimic the growth of the bubble and spike structure. The model has the strongest effect where the density gradients are strongest, scaled by the strength of gravity.

A limited investigation was performed with this model. Unfortunately, with a constant near unity the model effect was not sufficiently strong. Due to time limits other scalings were not tried. Possible improvements could include scaling with the Atwood number in addition to gravity, using horizontal instead of vertical gradients, or to attempt to correct for the fact that on coarse meshes, the density gradient used in the model is under-resolved.

4. Discussion and Conclusions

4.1. *Relevance to Fires*

The objective of both the experiments and simulations was to evaluate the coupling between the momentum source term and scalar fields in a flow relevant to fires. By studying non-reacting helium, both the scalar and momentum fields can be measured and the complications of combustion, soot formation, and radiation are avoided. As noted in the introduction, there are additional couplings in fires beyond the momentum source term coupling. Also, there are important differences between the helium plume and a reacting fire for the momentum source term. In the plume, the strongest gradients are at the base of the plume, and the mean driving force decreases with elevation as shown in Fig. 2. However, in a fire the gradients are not strongest between fuel and air but hot products and air, and the mean driving force first increases with elevation until the elevation of maximum combustion and then decreases. Most hydrocarbon fuel vapors are actually heavier than air and under these conditions, the fuel vapor is stably stratified. It is the high temperature products that are not stabily stratified and will show the development of RT instabilities. Thus, for heavier than air fuels, the fuel core (or vapor dome as it is sometimes referred to) will not necessarily be subject to RT bubbles and spikes like the helium plume.

Equations 3.2 and 3.3 suggest that as the Atwood number gets smaller (i.e., smaller density difference), the wavelength of the instability gets larger, and the growth rate of the bubble and spike structure slows down. Visualization of experiments by Tieszen *et al.* 2004 for methane and hydrogen fires qualitatively show this effect. Even though methane is buoyant relative to air, bubble and spike structure is almost not discernable in the movies. However, in hydrogen, the bubble and spike structure is much stronger than the helium plume, and the puffing is likewise much stronger.

These differences between reacting and non-reacting flows should be kept in mind for scaling studies. For example, for hydrocarbon fires, it may not be necessary to resolve the bubble and spike structure that may occur between the hot products and the air, because to leading order it does not affect the combustion rate of the fuel through enhanced mixing of the fuel vapors and air.

4.2. *Conclusions*

LES simulations, data for a one meter base diameter helium plume, and theoretical arguments are used to elucidate physics requirements for turbulent LES subgrid closure models for buoyant plumes. Both the data and highly resolved LES simulations show strong Rayleigh-Taylor (RT) instabilities that lead to turbulence and rapid scalar mixing near the base of strongly buoyant plumes. A grid refinement study using a dynamic Smagorinsky model shows strong grid dependency in the mean statistics, with the finest grid (4 million nodes) approaching the data. The authors interpret the temporally resolved results as indicating that the small scale RT structures play a significant role in the mean statistics. The authors argue that these structures must either be resolved or modeled to capture the mean statistics of the plume. In particular, it is noted that RT air spikes with O(mm-cm) widths have the ability to penetrate the plume source in the time-scale of the puffing frequency. The high radial entrainment at the plume base sweeps this air into the centerline of the plume at a very low elevation. The resulting relatively high mean-centerline-density moderates the mean driving force of the plume and results in centerline velocities that are about a factor of two lower than would occur if this mixing mode were not present.

4.3. *Acknowledgments*

Support for the lead author provided by Sandia, a multiprogram laboratory operated by Sandia Corporation, a Lockheed Martin Company, for the Untited States Department of Energy under Contract DE-AC04-94AL85000.

REFERENCES

CANUTO, V. M. 1994 Large Eddy Simulation of Turbulence: A Subgrid Scale Model Including Shear, Vorticity, Rotation, and Buoyancy, *Astrophysical J.* **158**:729-752.

CETEGEN, B. M. 1997 Measurements of Instantaneous Velocity Field of a Non-Reacting Pulsating Buoyant Plume by Particle Image Velocimetry, *Combust. Sci. and Tech*, **123**:377-87.

CETEGEN, B. M. & AHMED T. A. 1993 Experiments on the Periodic Instability of Buoyant Plumes and Pool Fires, *Combustion and Flame*,**93**:157-84.

DEBACQ, M., FANGUET, V., HULIN, J. P., & SALIN, D. 2001 Self-similar Concentration Profiles in Buoyant Mixing of Miscible Fluids in a Vertical Tube, *Phys. Fluids*,**13**(11):3097-3100.

DESJARDIN, P. E., O'HERN, T. J., & TIESZEN, S. R. 2004 Large Eddy Simulation and Experimental Measurements of the Near-Field of a Large Turbulent Helium Plume, *Phys. Fluids*,**16**(6):1866-1883.

DIMONTE, G., & SCHNEIDER, M. 2000 Density Ratio Dependence of Rayleigh -Taylor mixing, *Phys. Fluids*,**12**(2):304-321.

DRYSDALE, D. 1999 *An Introduction to Fire Dynamics, 2nd Ed.* John Wiley & Sons, NY, NY, p. 161.

DUFF, R. E., HARLOW, F. H., & HIRT, C. W. 1962 Effects of Diffusion on Interface Instability Between Gases, *Phys. Fluids*,**5**(4):417-425.

EIDSON, T. M. 1985 Numerical Simulation of the Turbulent Rayleigh-Benard Problem Using Subgrid Modeling. *J. Fluid Mech.*,**158**:245-268.

O'HERN, T. J., WECKMAN, E. J., GERHART, A. L., TIESZEN, S. R., & SCHEFER, R.

W. 2004 Experimental Study of a Turbulent Buoyant Helium Plume. *Manuscript in Review.*

MELL, W. E. 2001 Helium plume data available from author, National Institute of Standards and Technology, Building and Fire Research Laboratory, Gaithersburg, Maryland.

MELL, W. E., MCGRATTEN, K. B., & BAUM, H. R. 1996 Numerical Simulation of Combustion in Fire Plumes, *26th Symposium (International) on Combustion.* The Combustion Institute, pp. 2715-22.

NAJM, H. N., SCHEFER, R. B., MILNE, R. B., MUELLER, C. J., DEVINE, K. D., & KEMPKA, S. N. 1998 Numerical and Experimental Investigation of Vortical Flow-Flame Interaction. SAND98-8232 Sandia National Laboratories, Albuquerque, NM.

NICOLETTE, V. F., TIESZEN, S. R., BLACK, A. R., DOMINO, S. P., & O'HERN, T. J. 2004 A Turbulence Model for Buoyant Flows Based on Vorticity Generation. *Manuscript in Review.*

PIERCE, C. D. 2001 *Progress-variable Approach for Large Eddy Simulation of Turbulent Combustion.* Ph.D. Thesis, Stanford University.

PIERCE, C. D. & MOIN, P. 2004 Progress-variable Approach for Large Eddy Simulation of Non-premixed Turbulent Combustion. *J. Fluid Mech.*, **504**:73-97.

SOTERIOU, M. C., DONG, Y., & CETEGEN, B. M. 2002 Lagrangian Simulation of the Unsteady, Near Field Dynamics of Planar Buoyant Plumes, *Phys. Fluids*,**14**(9):3118-3140.

TIESZEN, S. R., NICOLETTE, V. F., GRITZO, L. A., HOLEN, J. K., MURRAY, D., & MOYA, J. L. 1996 Vortical Structures in Pool Fires: Observation, Speculation, and Simulation. SAND96-2607 Sandia National Laboratories, Albuquerque, NM.

TIESZEN, S. R. 2001 On the Fluid Mechanics of Fires, *Annu. Rev. Fluid Mech.*, **33**:67-92.

TIESZEN, S. R., DOMINO, S. P., & BLACK, A. R. 2004 Validation of a Simple Turbulence Model Suitable for Closure of Temporally-Filtered Navier-Stokes Equations Using a Helium Plume, Sandia National Laboratories, Albuquerque, NM In review.

TIESZEN, S. R., O'HERN, T. J., WECKMAN, E. J., & SCHEFER, R. W. 2004 Experimental Study of the Effect of Fuel Mass Flux on a One Meter Diameter Methane Fire and Comparison with a Hydrogen Fire, *Combustion and Flame* Accepted for publication.

WANG, C. 1984 *The Effects of Curvature on Turbulent Mixing Layers.* Ph.D. Thesis, California Institute of Technology.

XIN, Y., GORE, J., MCGRATTEN, K. B., REHM, R. G., & BAUM, H. R. 2002 Large Eddy Simulation of Pool Fires, *29th Symposium (International) on Combustion.* The Combustion Institute, pp. 259-265.